Nonaffine Strains Control Ductility of Metallic Glasses

Hui Wang, Wojciech Dmowski, Yang Tong, Zengquan Wang, Yoshihiko Yokoyama, Jittisa Ketkaew, Jan Schroers, and Takeshi Egami

Phys. Rev. Lett. **128**, 155501 — Published 15 April 2022

DOI: 10.1103/PhysRevLett.128.155501

Non-affine strains control ductility of metallic glasses

Hui Wang[1], Wojciech Dmowski[1], Yang Tong[1], Zengquan Wang[1], Yoshihiko Yokoyama[3], Jittisa Ketkaew[4], Jan Schroers[4], and Takeshi Egami[1, 2, 5]

[1]Department of Materials Science and Engineering, University of Tennessee, Knoxville, TN 37996 USA,
[2]Materials Science and Technology Division, Oak Ridge National Laboratory, Oak Ridge, TN 37831 USA,
[3] Institute for Materials Research, Tohoku University, 2-1-1 Katahira, Aoba-ku, Sendai 980-8577, Japan,
[4]Department of Mechanical Engineering & Materials Science, Yale University, New Haven, Connecticut 06511, USA
[5]Department of Physics and Astronomy, University of Tennessee, Knoxville, TN 37996 USA

Abstract

The origin of limited plasticity in metallic glasses is elusive, with no apparent link to their atomic structure. We propose that the response of the glassy structure to applied stress, not the original structure itself, provides a gauge to predict the degree of plasticity. We carried out high-energy x-ray diffraction on various BMGs under uniaxial compression within elastic limit and evaluated the anisotropic pair distribution function. We show that the extent of local deviation from the affine (uniform) deformation in the elastic regime is strongly correlated with the plastic behavior of BMGs beyond yield, across chemical compositions and sample history. The results suggest that the propensity for collective local atomic rearrangements under stress promotes plasticity.

Bulk metallic glasses exhibit high strength and high elastic limit with potential for structural applications [1,2,3]. On the other hand, the fracture toughness varies widely from those exhibiting exceptional tough behavior [4], to others showing close to ideal brittle behavior [5]. It had been observed that ductile BMGs exhibit a low ratio of shear modulus/bulk modulus [6] and a direct correlation of ductility with this ratio was suggested [5]. However, follow-up research revealed that such correlation does not exist across the different chemical compositions [7,8,9]. Attempts to relate the plasticity to the atomic structure of glass have been mostly indirect [10,11], because it is difficult to define direct structural feature or parameter related to ductility such as "defects" in crystals. The leading model of mechanical deformation in metallic glasses is the shear-transformation-zone (STZ) model [12–14]. The STZs are local events involving 5 – 50 atoms [15,16], which undergo atomic rearrangements during deformation. STZs are not pre-existing defects but emerge upon deformation and disappear afterwards [13,15,16]. Therefore, STZ cannot be detected by examining the structure prior to deformation, unlike dislocations in crystals. Some attempts have been made to relate the initial structure to propensity of deformation, using MD [17] or through machine learning [18,19]. However, they are only partially successful, and are not amenable for experimental verification.

On the other hand, the change in the structure under stress could provide relevant information regarding the deformation mechanism. It is recognized that at the atomic level the deformation of glass is not uniform, and stress induces locally non-affine atomic displacements even in the elastic regime [20–24]. Therefore "elastic regime" is not strictly elastic, but we use this term to describe macroscopic deformation range before yielding. Simulation in the two-dimensional Lennard-Jones system suggests local non-affine modulus is related to plastic events [25]. In this work, we show that the extent of local deviations from the affine deformation in the elastic regime is strongly correlated with the plastic behavior of BMGs upon yielding at higher stresses. We propose a parameter, the local non-affine strain ratio, $\Delta\varepsilon_R/\varepsilon_\infty$, to quantify the local structural response to the applied stress in the elastic regime. This characterization represents a predictive method to assess plasticity across different chemistry of BMGs and provides new perspective on the deformation mechanism.

We carried out in situ high-energy x-ray diffraction measurements on various BMGs under uniaxial compression at the beamline 1-ID of the Advanced Photon Source (APS), Argonne National Laboratory to characterize non-affine strains. (For experimental details see Supplemental

Material [26]). Under uniaxial stress the structure of the glass becomes anisotropic. The isotropic and anisotropic components of the pair distribution function (PDF) were obtained as a function of applied stress:

$$g(r,\chi) = g_0^0(r) + \sqrt{5}P_2^0(\cos\chi)g_2^0(r) \quad (1)$$

Here χ is an angle between the $\boldsymbol{r}$ and the z-axis, which is aligned with the stress direction, $P_l^m(x)$ is the associated Legendre polynomial, and $r = |\boldsymbol{r}|$. The elliptic term ($m = 0$, $l = 2$) measures the anisotropy of the glass and is related to the strain. It was shown before [31] that if the elastic deformation is affine the anisotropic component of the PDF is related to the derivative of the isotropic PDF as shown in Figure 1 (a):

$$\rho_0 g_{2,exp}^0(r) = \pm\varepsilon_{affine}\frac{2(1+\nu)}{3\sqrt{5}} r\frac{d}{dr}\rho_0 g_0^0(r) \quad (2)$$

Here ρ_0 is the number density of atoms, ν is Poisson's ratio, ε_{affine} is the amplitude of affine strain. The "±" signs indicate compression and tension, respectively. However, deformation in a glass is heterogeneous at the atomic level even in the elastic regime, because of the spatial variation in elastic modulus and local strain relaxation, which results in a non-affine length-scale dependent

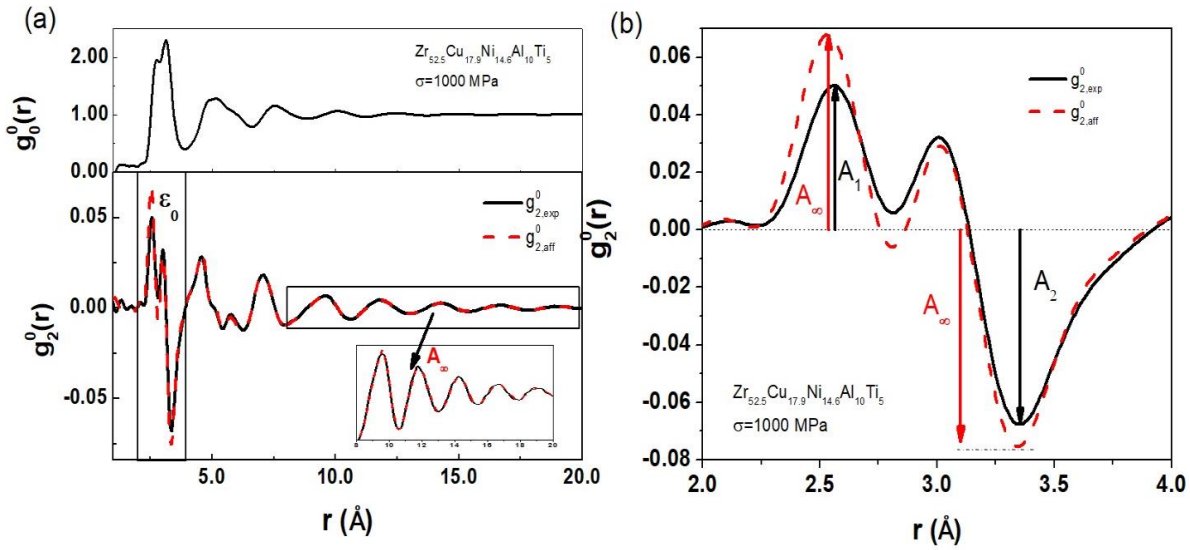

Figure 1. (a) The isotropic PDF (top); and (bottom) the fitting of the anisotropic PDF with the derivative of the isotropic PDF (affine anisotropic PDF) to obtain affine strain ε_∞. The red broken curve represents the "expected" or affine $g_2^0(r)$ basing on a derivative of $g_0^0(r)$. (b) Amplitudes A_i in the short range of anisotropic PDF to obtain local strains $\varepsilon_1, \varepsilon_2$ (eq. 3).

strain, $\varepsilon(r)$, which substitutes constant, affine strain, in eq. (2). Specifically, the local strain in the first atomic shell is smaller than the expected long-range strain, as is illustrated in the Figure 1 (b). The long-range strain obtained by fitting eq. (2) at large distances is plotted as a red dashed line. The eq. (2) with r-dependent strain, $\varepsilon(r)$, can be used in evaluating the strain in two ranges of distance: in the first atomic shell and beyond as shown in Figure 1 (b). In this equation, both $\rho_0 g_2^0(r)$ and $\rho_0 g_0^0(r)$ are determined independently from the experiment.

The fitting by eq. (2) works well at long-r range (~ 6 - 20 Å) indicating that the strain beyond the second shell is equal to the long-range average strain. The long-range strain, ε_∞, obtained from this fit defines the reference state for each measurement. For the first atomic shell, the $\varepsilon(r)$ is smaller than the affine ε_{affine} predicted by eq. (2). This deviation is commonly observed in the elastic deformation of all the BMG samples we measured. The reduced amplitude of the $\varepsilon(r)$ in the first shell indicates that the local strain is smaller than the long-range average strain suggesting that local strain relaxation occurs under applied stress even in the elastic regime. Thus, we can use the difference between the long-range strain and the local strain as a measure of the capacity of glass to relax the stress by local atomic rearrangements under load.

Because $g_2^0(r)$ is proportional to the derivative of $g_0^0(r)$ as given in eq. (2), the first peak of $g_0^0(r)$ corresponds to a pair of positive and negative peaks in $g_2^0(r)$. The local strain was evaluated by taking the average of the strains for the positive and negative peaks, ε_1 and ε_2, defined by,

$$A_i = \varepsilon_i \cdot \frac{2(1+\nu)}{3\sqrt{5}} r_i \frac{d}{dr} g_0^0(r_i);\ i = 1,2 \tag{3}$$

where A_1 and r_1 are the height and position of the first positive peak, and A_2 and r_2 are the height and position of the negative peak. The extent of local strain relaxation is expressed by the ratio, $\Delta\varepsilon_R/\varepsilon_\infty$, as defined below. The denominator, ε_∞, is the long-range average strain obtained from fitting the eq. (2) in large-r range. The numerator, $\Delta\varepsilon_R$, is the amount of the relaxed strain, i.e., the difference between the long-range and the local strain. Thus, $\Delta\varepsilon_R = \varepsilon_\infty - (\varepsilon_1 + \varepsilon_2)/2$.

The $\Delta\varepsilon_R$ and ε_∞ are dependent on the applied stress as is shown in Fig S2 (Supplementary Material [26]). However, their ratio $\Delta\varepsilon_R/\varepsilon_\infty$ is nearly independent of stress as shown in Fig. S3 [26] for several glass compositions appearing as macroscopic linear anelasticity. This confirms that the local non-affine strain ratio is an intrinsic parameter characterizing the ability of the glass

to relax strain locally, and it justifies the comparison of $\Delta\varepsilon_R/\varepsilon_\infty$ for different BMGs measured at slightly different stresses.

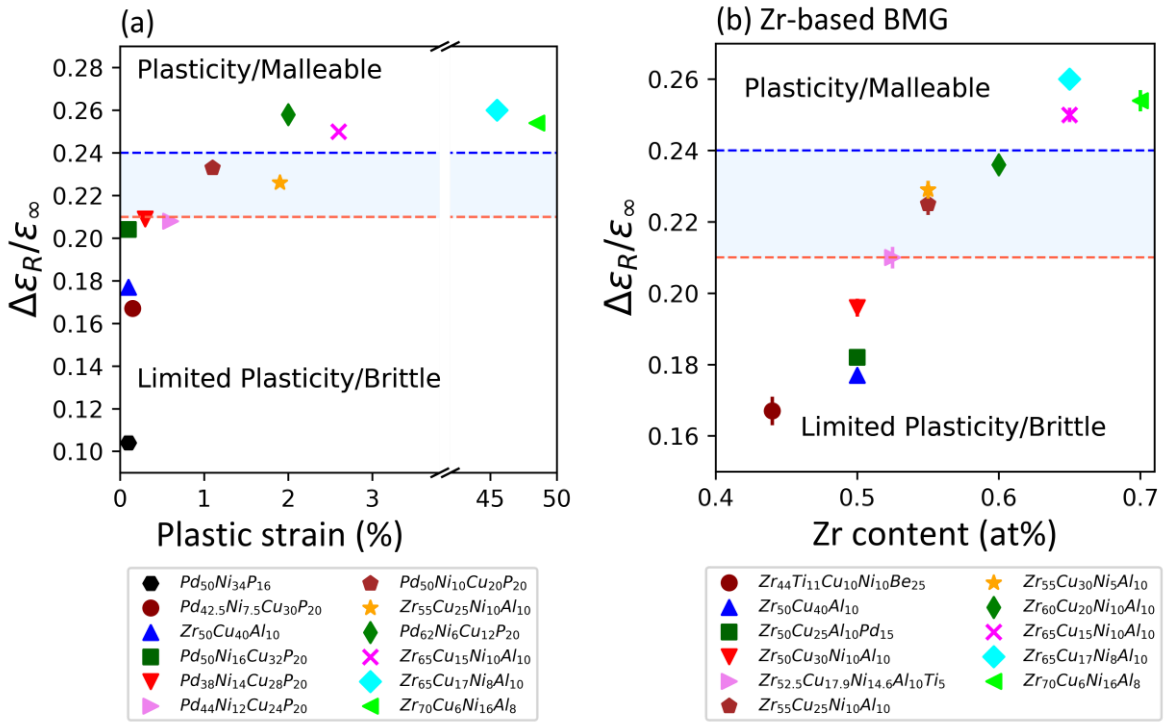

Figure 2. (a) The non-affine strain relaxation ratio as function of a plastic strain for several Zr and Pd-based BMGs. (b) The non-affine strain ratio for Zr-based BMG. Error bars are vertical streaks typically the size of the symbol data point.

The mechanical properties of Zr-based BMG have been studied extensively e.g., [32–34]. The Zr rich compositions tend to show more plasticity in compression tests and exhibit higher fracture toughness [35,36,37], and show plastic strains even in tension [37]. This trend has been attributed to the increasing value of the Poisson's ratio with Zr content [5,38]. The change in the local non-affine strain ratio, $\Delta\varepsilon_R/\varepsilon_\infty$, for several Zr- and Pd-based BMGs is shown in Figure 2(a) as function of the plastic strain after yielding (See Figure S4 in Supplemental Material [26]). The plot, despite some scatter, shows that glasses with large $\Delta\varepsilon_R/\varepsilon_\infty$ ratio tend to exhibit large plastic strains, whereas glasses with a small strain ratio have small plastic strains and/or fracture in a brittle manner. This behavior is illustrated by the compression mechanical tests on $Zr_{50}Cu_{40}Al_{10}$ and $Zr_{65}Cu_{17}Ni_8Al_{10}$ as shown in Figure S4 (a) and in Fig 2: $Zr_{50}Cu_{40}Al_{10}$ with small $\Delta\varepsilon_R/\varepsilon_\infty$ (=

0.177) shows very limited plasticity, whereas $Zr_{65}Cu_{17}Ni_8Al_{10}$ with large $\Delta\varepsilon_R/\varepsilon_\infty$ (= 0.26) exhibits large plastic strains and is malleable (more than 50% plastic strain). The results in Fig 2(a) demonstrate that the local strain ratio is a good indicator of plasticity of BMGs. The extensive literature data on the plastic behavior of different Zr-based BMGs allows us to establish general correlation of the local non-affine strain ratio with plasticity. Based on the reported mechanical behaviors [5,7,37–39] and our measurements, we conclude that the range of the value of $\Delta\varepsilon_R/\varepsilon_\infty$, 0.21 – 0.24, separates ductile behavior from brittle one as is shown in Fig. 2(b) for the Zr-based BMGs. The upper limit of ~0.24 is based on the result that the Zr-based BMGs with $\Delta\varepsilon_R/\varepsilon_\infty$ above 0.24 show large plasticity in compression tests and are malleable, and they even show some plastic strains in tension [37,39]. The plastic behavior in tension is exceptional and indicative of intrinsic ductility of these compositions. We suggest that this plastic response is related to large non-affine strains observed in our x-ray experiment and quantified by the large strain ratio that reflects the ability of the glass to relax strain locally. However, when $\Delta\varepsilon_R/\varepsilon_\infty$ is below 0.21, the Zr-based glasses either show limited plasticity in compression or break in a brittle manner right away upon yielding. The reported experimental plastic strains for glasses with $\Delta\varepsilon_R/\varepsilon_\infty$ between 0.21 and 0.24 vary in literature due to scatter in sample quality and testing conditions. However, they clearly imply that plasticity is rather limited. The results in Fig. 2(b) show that Zr-based glasses for which the $\Delta\varepsilon_R/\varepsilon_\infty$ ratio is below 0.21 are brittle, whereas those with the $\Delta\varepsilon_R/\varepsilon_\infty$ ratio above 0.24 are ductile.

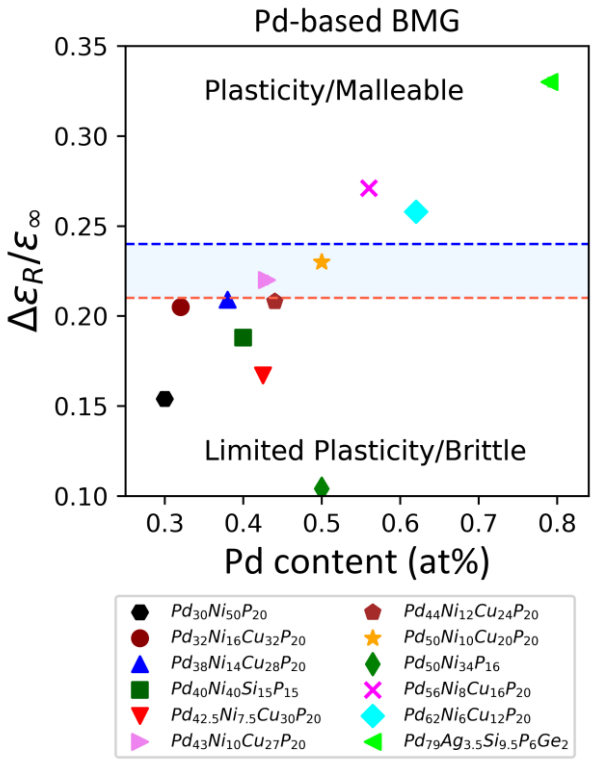

Figure 3. The ratio of relaxed strain to the long-range strain for Pd-based BMG. Error bars are black vertical streaks typically the size of the circle data point.

The local non-affine strain ratio, $\Delta\varepsilon_R/\varepsilon_\infty$, for different Pd-based BMGs are presented by symbols with different colors in Figure 3. In assessing plasticity, the available mechanical data [8] are combined with our own compression tests. The stress-strain curves from our compression tests on some of these Pd-based glasses are presented in Supplement Material Fig. S4(b) [26]. Generally, glasses with small $\Delta\varepsilon_R/\varepsilon_\infty$, below ~ 0.21, such as $Pd_{42.5}Ni_{7.5}Cu_{30}P_{20}$ ($\Delta\varepsilon_R/\varepsilon_\infty = 0.17$), $Pd_{32}Ni_{16}Cu_{32}P_{20}$ ($\Delta\varepsilon_R/\varepsilon_\infty = 0.20$, $Pd_{50}Ni_{34}P_{16}$ ($\Delta\varepsilon_R/\varepsilon_\infty = 0.104$), $Pd_{38}Ni_{14}Cu_{28}P_{20}$ ($\Delta\varepsilon_R/\varepsilon_\infty = 0.21$), and $Pd_{44}Ni_{12}Cu_{24}P_{20}$ ($\Delta\varepsilon_R/\varepsilon_\infty = 0.21$) show brittle or very limited plastic strains. The $Pd_{79}Ag_{3.5}P_6Si_{9.5}Ge_2$ ($\Delta\varepsilon_R/\varepsilon_\infty = 0.33$) has an exceptionally large value of $\Delta\varepsilon_R/\varepsilon_\infty$. The reported data for $Pd_{79}Ag_{3.5}P_6Si_{9.5}Ge_2$ [4] shows extreme fracture toughness with large plastic flow before cavitation. This glass was termed damage tolerant, and its behavior is consistent with the largest value of $\Delta\varepsilon_R/\varepsilon_\infty$ we measured. The available data combined with ours confirms the conclusion, suggested for Zr-based glasses, that large non-affine strain ratio parameter, $\Delta\varepsilon_R/\varepsilon_\infty > 0.24$, correlates with intrinsic plasticity.

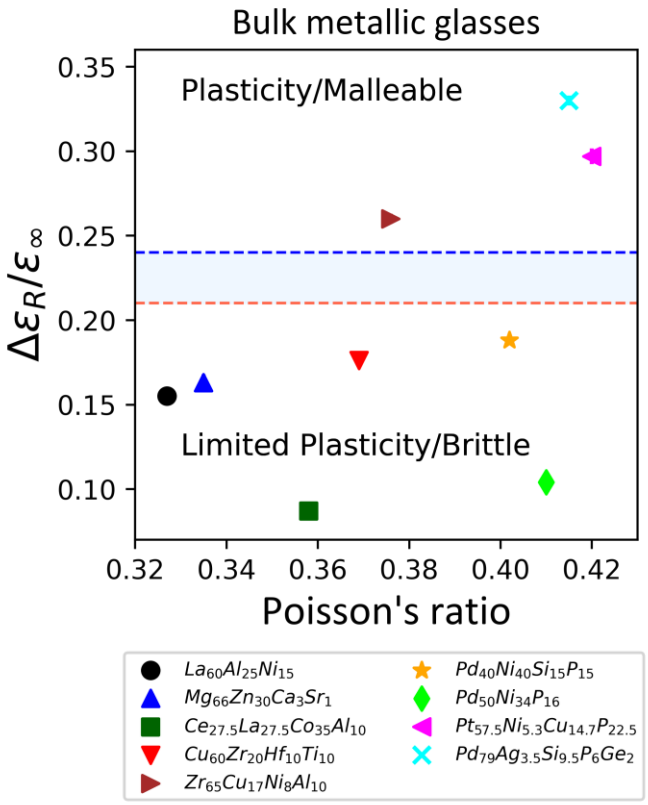

Figure 4. The non-affine strain ratio for different BMGs with Poisson's ratio larger than 0.32. Vertical bars indicate error.

Local non-affine strain ratio is also measured for other BMGs and displayed in Figure 4 together with some Zr and Pd alloys against Poisson's ratio, ν. It was suggested that BMGs with increasing ν exhibit larger plasticity and tend to be ductile when ν is above 0.32 [11]. Poisson's ratios of all the BMGs in Figure 4 are above 0.32. Nevertheless, among them, $La_{60}Al_{25}Ni_{15}$, $Mg_{66}Zn_{30}Ca_3Sr_1$, $Ce_{27.5}La_{27.5}Co_{35}Al_{10}$, $Cu_{60}Zr_{20}Hf_{10}Ti_{10}$ and $Pd_{50}Ni_{34}P_{16}$ are brittle according to the reported mechanical tests [8,40,41,42,43]. The brittle behavior of these BMGs is tracked very well by their

small local non-affine strain ratio with values well below 0.21. On the other hand, $Zr_{65}Cu_{17}Ni_8Al_{10}$, $Pt_{57.5}Cu_{14.7}Ni_{5.3}P_{22.5}$ and $Pd_{79}Ag_{3.5}P_6Si_{9.5}Ge_2$ have the value of $\Delta\varepsilon_R/\varepsilon_\infty$ above 0.24 and exhibit large plasticity [4,6,37]. Figure 4 indicates that the RT plastic behavior of various BMGs does not correlate with Poisson's ratio, and in contrast, it correlates quite well with the local non-affine strain ratio $\Delta\varepsilon_R/\varepsilon_\infty$. It appears that the transition range of $\Delta\varepsilon_R/\varepsilon_\infty$, 0.21 – 0.24, separates the brittle behavior below and ductile behavior above universally for various glassy compositions.

It is known that thermal history has significant influence on the mechanical behavior of BMGs. For instance, the cooling rate directly affects the state of BMG by changing its fictive temperature, T_f, and thus its glassy structure [10,44,45]. Annealing [9,46] and thermo-mechanical creep [47,48] can modify T_f, moving glass to a more relaxed, or to a rejuvenated state. Supplement Figure S5 [26] shows that the local non-affine strain ratio, $\Delta\varepsilon_R/\varepsilon_\infty$, tracks changes in the fictive temperature for a glass with the same composition. These data confirm that non-affine strain ratio is an intrinsic parameter and connects to plasticity of metallic glasses.

Our results show that the local non-affine strain ratio, characterizing the response of the local structure of BMG to external stress, is an indicator of compressive plasticity across BMGs of different alloy systems. Even though the *G/B* ratio correlates with plasticity or toughness within a limited range for each alloy system [5,11,49], it fails for BMGs of different alloy systems [7,50]. The independence of the $\Delta\varepsilon_R/\varepsilon_\infty$ of the magnitude of the applied stress validates that it is an intrinsic property of a BMG controlled by its chemical composition and its fictive temperature. The local non-affine strain ratio measures the extent of atomic rearrangements induced by external stress. Therefore, it is not surprising that it relates to the potential of plastic deformation. Indeed, as seen in Figures 2, 3 and 4, typical brittle BMGs have very small $\Delta\varepsilon_R/\varepsilon_\infty$ ratios whereas samples showing plasticity have large ones.

It was observed that the application of stress below the apparent elastic limit results in local "plastic" deformation, or local topological relaxation (LTR), by cutting or forming local atomic bonds [24,51]. Such local changes in the topology of atomic connectivity [52,53], are most likely the origin of the observed $\Delta\varepsilon_R/\varepsilon_\infty$ ratio. At low stress levels such bond cutting and forming events are low in density and are well separated both in time and space. Each one of them is locally constrained by the elastic medium around them, contributing to internal friction [54]. At higher stress levels several contiguous events of bond rearrangement occur, involving typically five atoms [55], emerging as STZs. A simulation study [56] suggests that the occurrence of cascade STZs is

linked to ductile behavior. If the stress concentration at the crack tip can be relaxed by a high density of induced STZs the crack tip can be blunted, and mechanical failure can be avoided. Thus, the local non-affine strain ratio, $\Delta\varepsilon_R/\varepsilon_\infty$, probes the capability of the glass to accommodate local shear strain to promote STZs, leading to plastic flow [55]. The sensitivity of the value of $\Delta\varepsilon_R/\varepsilon_\infty$ to thermal history suggests a strong link between this ratio and the density, or propensity of STZ [57]. A high value of $\Delta\varepsilon_R/\varepsilon_\infty$ means easier local atomic rearrangement upon application of stress, leading to the formation of STZ at yielding.

The quantification of ductility or plasticity in metallic glasses is a daunting task by itself. Ideally, a standard fracture toughness test should be used [58]. However, preparing BMG samples fulfilling such requirements, the size in particular, is not feasible for the wide range of BMGs considered in this research. Therefore, to assess the correlation of our parameter with plasticity in metallic glasses we chose to use simple compression tests allowing use of small samples to examine many glassy compositions.

In summary, we have identified the local non-affine strain ratio, which quantifies the non-affine strains and controls the capacity for local strain relaxation, as a best predictor for compressive plasticity in BMGs. This ratio is independent of the applied stress and depends only on the composition and fictive temperature. This parameter may be related to the propensity for creating shear-transformation-zones. Whereas it is difficult, if possible, at all, to determine such propensity from the structure itself, the local non-affine strain ratio can be measured straightforwardly and provides excellent prediction of the plasticity of BMG under compressive stress.

Acknowledgement.

This work was supported by the U. S. Department of Energy, Office of Science, Basic Energy Sciences, Materials Sciences and Engineering Division. We would like to thank 1-ID beamline team at APS for assistance with x-ray experiment. The Advanced Photon Source, a U.S. Department of Energy (DOE) Office of Science User Facility is operated for the DOE Office of Science by Argonne National Laboratory under Contract No. DE-AC02-06CH11357.

Data availability

All data included in this work are available upon request to the corresponding author.

References

[1] A. Inoue, B. Shen, H. Koshiba, H. Kato, and A.R. Yavari, Cobalt-based bulk glassy alloy with ultrahigh strength and soft magnetic properties, Nat. Mater. **2,** 661 (2003).

[2] M.F. Ashby and A.L. Greer, Metallic glasses as structural materials, Scr. Mater. **54,** 321 (2006).

[3] L. Tian, Y. Q. Cheng, Z. W. Shan, J. Li, C. C. Wang, X. D. Han, J. Sun, and E. Ma, Approaching the ideal elastic limit of metallic glasses, Nature Commun. **3,** 609 (2012).

[4] M. D. Demetriou, M.E. Launey, G. Garrett, J.P. Schramm, D.C. Hofmann, W.L. Johnson, and R.O. Ritchie, A damage-tolerant glass, Nat. Mater. **10,** 123 (2011).

[5] J.J. Lewandowski, W.H. Wang, and A.L. Greer, Intrinsic plasticity or brittleness of metallic glasses, Phil. Mag. Lett., **85**, 77 (2005).

[6] J. Schroers and W.L. Johnson, Ductile bulk metallic glass, Phys. Rev. Lett., **93**, 255506 (2004).

[7] G. Kumar, D. Rector, R.D. Conner, and J. Schroers, Embrittlement of Zr-based bulk metallic glasses, Acta Mater., **57**, 3572 (2009).

[8] G. Kumar, S. Prades-Rodel, A. Blatter, and J. Schroers, Unusual brittle behavior of Pd-based bulk metallic glass, Scr. Mater., **65**, 585 (2011).

[9] J. Ketkaew, W. Chen, H. Wang, A. Datye, M. Fan, G. Pereira, U.D. Schwarz, Z. Liu, R. Yamada, W. Dmowski, et al. Mechanical glass transition revealed by the fracture toughness of metallic glasses, Nat. Commun. **9,** 3271 (2018).

[10] K. Golden, P. Neibecker, Y.H. Liu, and J. Schroers, Critical fictive temperature for plasticity in metallic glasses, Nature Commun. **4,** 1536 (2013).

[11] S. V. Madge, D.V. Louzguine-Luzgin, J.J. Lewandowski, and A.L. Greer, Toughness, extrinsic effects and Poisson's ratio of bulk metallic glasses, Acta Mater. **60,** 4800 (2012).

[12] A.S. Argon, Plastic deformation in metallic glasses, Acta Metall. **27,** 47 (1979).

[13] A.S. Argon and L.T. Shi, Development of visco-plastic deformation in metallic glasses, Acta Metall. **31,** 499 (1983).

[14] J.S. Harmon, M.D. Demetriou, W.L. Johnson, and K. Samwer, Anelastic to plastic transition in metallic glass-forming liquids, Physical Review Letters **99,** 135502 (2007).

[15] Y. Fan, T. Iwashita, and T. Egami, How thermally activated deformation starts in metallic glass, Nature Commun. **5,** 5083 (2014).

[16] I.C. Choi, Y. Zhao, Y.J. Kim, B.G. Yoo, J.Y. Suh, U. Ramamurty, and J.I. Jang, Indentation size effect and shear transformation zone size in a bulk metallic glass in two different structural states, Acta Mater. **60,** 6862 (2012).

[17] J. Ding, Y.-Q. Cheng, H. Sheng, M. Asta, R. O. Ritchie and E. Ma, Universal structural parameter to quantitatively predict metallic glass properties, Nat. Commun. 7, 13733 (2016).

[18] E. D. Cubuk, S. S. Schoenholz, J. M. Rieser, B. D. Malone, J. Rottler, D. J. Durian, E. Kaxiras, and A. J. Liu, Identifying structural flow defects in disordered solids using machine-learning methods, Phys. Rev. Lett. **114**, 108001 (2015).

[19] V. Bapst, T. Keck, A. Grabska-Barwińska, C. Donner, E. D. Cubuk, S. S. Schoenholz, A. Obika, A. W. R. Nelson, T. Back, D. Hassabis & P. Kohli, Unveiling the predictive power of static structure in glassy systems, Nature Phys. **16**, 448-454 (2020).

[20] D. Weaire, M.F Ashby, J. Logan, and J. Weis, On the use of pair potentials to calculate the properties of amorphous metals, Acta Metall. **19,** 779 (1971).

[21] H.F. Paulsen, J.A. Wert, J. Neuefeind, V. Honkimaki, and M. Daymond, Measuring strain distributions in amorphous materials, Nature Mater. **4,** 33 (2005).

[22] T.C. Hufnagel, R.T. Ott, and J. Almer, Structural aspects of elastic deformation of a metallic glass, Phys. Rev. B **73,** 064204 (2006).

[23] W. Dmowski, T. Iwashita, C.P. Chuang, J. Almer, and T. Egami, Elastic heterogeneity in metallic glasses, Phys. Rev. Lett. **105,** 205502 (2010).

[24] T. Egami, T. Iwashita, and W. Dmowski, Mechanical properties of metallic glasses, Metals **3,** 77 (2013).

[25] B. Xu, M. L. Falk, S. Patinet and P. Guan, Atomic nonaffinity as a predictor of plasticity in amorphous solids, Phys. Rev. Mat. **5**, 025603 (2021).

[26] See Supplemental Material at [URL] for details on sample preparation, high energy x-ray diffraction and deformation data, which includes Refs. [27–30]

[27] Y. Yokoyama, K. Inoue, and K. Fukaura, Pseudo Float Melting State in Ladle Arc-Melt-Type Furnace for Preparing Crystalline Inclusion-Free Bulk Amorphous Alloy, Mater. Trans. **43**, 2316 (2002).

[28] A.P. Hammersley, S.O. Svensson, A. Thompson, H. Graafsma, Å. Kvick, J.P. Moy, Calibration and correction of distortions in 2D detector systems, Rev. Sci. Instr. (SRI-94) **66**, 2729 (1995).

[29] T. Egami, Y. Tong, and W. Dmowski, Deformation in Metallic Glasses Studied by Synchrotron X-Ray Diffraction, Metals, **6**, 22 (2016).

[30] B.H. Toby and T. Egami, Accuracy of pair distribution function analysis applied to crystalline and non-crystalline materials, Acta Cryst. **A48**, 336 (1992).

[31] Y. Suzuki, J. Haimovich, and T. Egami, Bond-orientational anisotropy in metallic glasses observed by x-ray diffraction, Phys. Rev. B **35,** 2162 (1987).

[32] H.A. Bruck, A.J. Rosakis, and W.L. Johnson, The dynamic compressive behavior of beryllium bearing bulk metallic glasses, J. Mater. Res. **11**, 503 (1996).

[33] L.Y. Chen, Z.D. Fu, G.Q. Zhang, X.P. Hao, Q.K. Jiang, X.D. Wang, Q.P. Cao, H. Franz, Y.G. Liu, H.S. Xie, et al., New class of plastic bulk metallic glass, Phys. Rev. Lett. **100,** 075501 (2008).

[34] C.T. Liu, L. Heatherly, J. A. Horton, D.S. Easton, C.A. Carmichael, J.L. Wright, J.H. Schneibel, M.H. Yoo, C.H. Chen, and A. Inoue, Test environments and mechanical properties of Zr-base bulk amorphous alloys, Metall. Mater. Trans. A **29**, 1811 (1998).

[35] Z. Bian, G.L. Chen, G. He, and X.D. Hui, Microstructure and ductile–brittle transition of as-cast Zr-based bulk glass alloys under compressive testing, Mater. Sci. Eng. A **316**, 135 (2001).

[36] C. Fan, C.F. Li, A. Inoue, and V. Haas, Deformation behavior of Zr-based bulk nanocrystalline amorphous alloys, Phys. Rev. B **61**, R3761 (2000).

[37] Y. Yokoyama, K. Fujita, A.R. Yavari, and A. Inoue, Malleable hypoeutectic Zr–Ni–Cu–Al bulk glassy alloys with tensile plastic elongation at room temperature, Phil. Mag. Lett. **89,** 322 (2009).

[38] G.Y. Wang, P.K. Liaw, Y. Yokoyama, A. Peker, W.H. Peter, B. Yang, M. Freels, Z.Y. Zhang, V. Keppens, R. Hermann, et al., Studying fatigue behavior and Poisson's ratio of bulk-metallic glasses, Intermetallics **15**, 663 (2007).

[39] Y. Yokoyama, M. Yamada, T. Mori, H. Tokunaga, T. Sato, T. Shima, M. Nishijima, K. Fujita, and T. Yamasaki, Solid plasticity and supercooled-liquid thermoplasticity of Zr-Cu-enriched hypoeutectic Zr-Cu-Ni-Al cast glassy alloys, Mater. Sci. & Eng. A **606**, 74 (2014).

[40] Q. Wang, J.J. Liu, Y.F. Ye, T.T. Liu, S. Wang, C.T. Liu, J. Lu, and Y. Yang, Universal secondary relaxation and unusual brittle-to-ductile transition in metallic glasses, Mater. Today **20,** 293 (2017).

[41] S.V. Madge, P. Sharma, D.V. Louzguine-Luzgin, A.L. Greer, and A. Inoue, New La-based glass–crystal ex situ composites with enhanced toughness, Scr. Mater. **62**, 210 (2010).

[42] Y.Y Zhao, E. Ma, and J. Xu, Reliability of compressive fracture strength of Mg–Zn–Ca bulk metallic glasses: Flaw sensitivity and Weibull statistics, Scr. Mater. **58**, 496 (2008).

[43] J. He, N. Mattern, I. Kaban, F. Dai, K. Song, Z. Yan, J. Zhao, D. H. Kim, and J. Eckert, Enhancement of glass-forming ability and mechanical behavior of zirconium–lanthanide two-phase bulk metallic glasses, J. Alloy Compd. **618**, 795 (2015).

[44] A. Q. Tool, Relation between inelastic deformability and thermal expansion of glass in its annealing range, J. Am. Ceram. Soc. **29**, 240 (1946).

[45] S.S. Tsao and F. Spaepen, Effects of annealing on the isoconfigurational flow of a metallic glass, Acta Metall. **33**, 891 (1985).

[46] Y. Yokoyama, T. Yamasaki, P.K. Liaw, and A. Inoue, Study of the structural relaxation-induced embrittlement of hypoeutectic Zr–Cu–Al ternary bulk glassy alloys, Acta Mater. **56**, 6097 (2008).

[47] Y. Tong, W. Dmowski, Y. Yokoyama, G. Wang, P.K. Liaw, and T. Egami, Recovering compressive plasticity of bulk metallic glasses by high-temperature creep, Scr. Mater. **69**, 570 (2013).

[48] Y. Tong, T. Iwashita, W. Dmowski, H. Bei, Y. Yokoyama, and T. Egami, Structural rejuvenation in bulk metallic glasses, Acta Mater. **86**, 240 (2015).

[49] W.H. Wang, Correlations between elastic moduli and properties in bulk metallic glasses, J. Appl. Phys., **99**, 093506 (2006).

[50] N. Nollmann, I. Binkowski, V. Schmidt, H. Rösner, and G. Wilde, Impact of micro-alloying on the plasticity of Pd-based bulk metallic glasses. Scr Mater. **111**, 119 (2016).

[51] Y. Suzuki and T. Egami, Shear deformation of glassy metals: breakdown of Cauchy relationship and anelasticity, J. Non-Cryst. Solids **75**, 361 (1985).

[52] T. Egami, Elementary Excitation and Energy Landscape in Simple Liquids, Mod. Phys. Lett. B, **28,** 1430006 (2014).

[53] T. Iwashita, D.M. Nicholson, and T. Egami, Elementary excitations and crossover phenomenon in liquids, Phys. Rev. Lett. **110**, 205504 (2013).

[54] N. Morito and T. Egami, Internal Friction and reversible structural relaxation in the Metallic Glass Fe32Ni36Cr14P12B6, Acta metal. **32**, 603 (1984).

[55] J. Bellissard and T. Egami, Simple theory of viscosity in liquids, Phys. Rev. E **98**, 063005 (2018).

[56] Y. Fan, T. Iwashita, and T. Egami, Crossover from Localized to Cascade Relaxations in Metallic Glasses, Phys. Rev. Lett. **115**, 045501 (2015).

[57] J.S. Langer, Shear-transformation-zone theory of plastic deformation near the glass transition, Phys. Rev. E **77**, 021502 (2008).

[58] W. Chen, H. Zhou, Z. Liu, J. Ketkaew, L. Shao, P. Gong, W. Samela, H. Gao, and J. Schroers, Test sample geometry for fracture toughness measurements of bulk metallic glasses, Acta Mater., **145**, 477 (2018).